Singular Arc Time-Optimal Climb Trajectory of Aircraft in a Two-Dimensional Wind Field

Nhan Nguyen*

NASA Ames Research Center, Moffett Field, CA 94035

This paper presents a study of a minimum time-to-climb trajectory analysis for aircraft flying in a two-dimensional altitude dependent wind field. The time optimal control problem possesses a singular control structure when the lift coefficient is taken as a control variable. A singular arc analysis is performed to obtain an optimal control solution on the singular arc. Using a time-scale separation with the flight path angle treated as a fast state, the dimensionality of the optimal control solution is reduced by eliminating the lift coefficient control. A further singular arc analysis is used to decompose the original optimal control solution into the flight path angle solution and a trajectory solution as a function of the airspeed and altitude. The optimal control solutions for the initial and final climb segments are computed using a shooting method with known starting values on the singular arc. The numerical results of the shooting method show that the optimal flight path angle on the initial and final climb segments are constant. The analytical approach provides a rapid means for analyzing a time optimal trajectory for aircraft performance.

I. Introduction

The climb performance of an aircraft is an important design requirement for establishing trajectories to reach a specified altitude and airspeed after takeoff in some optimal manner. For transport aircraft, a climb segment may follow a trajectory designed to achieve an optimal fuel consumption or a minimum time. Trajectory optimization problems to minimize aircraft fuel consumption or time of climb had been studied by various contributors in the 70's and 80's.[1–7] In recent years, minimum time problems have also been examined for many space systems.[8–10] Many approaches are found in literature for analyzing optimal flight trajectories for a minimum time-to-climb of an aircraft. One such method is based on the singular perturbation method that has been investigated for the minimum time-to-climb problem.[3,5] The singular perturbation method performs a time-scale separation of the fast and slow states in flight dynamic equations so that the dimension of the problem is reduced by the order of the fast states. If the aircraft is modeled as a point mass with three state variables: altitude, speed, and flight path angle, then the flight path angle is considered as a fast state and therefore its differential equation can be treated in a quasi-steady state approximation.[14] This allows the flight path angle be treated as a control variable for the minimum time optimal control problem.

Another popular method is based on the energy state approximation method,[1,4,6] which facilitates a simple means for computation by combining the altitude and speed variables into the energy state variable that represents the sum of the kinetic energy and potential energy of the aircraft during climb. Because of the order reduction in the state equations, the energy state approach enjoyed a popularity in minimum time optimal control problems. The total energy level curves thus can be viewed as curves of sub-optimal climb path.[11] Climbs or dives along the energy level curves theoretically is supposed to take virtually little time. In some climb maneuvers, an aircraft often has to execute an energy dive to trade altitude for speed. Once a desired speed is attained, the aircraft climbs out of the current energy level curve and transitions into a curve that takes the aircraft to the next energy level curve. This transition curve cuts across the energy level curves in an optimal manner such that the altitude can be gained in a minimum time. This curve is known as the energy climb path. Fig. 1 illustrates an energy climb maneuver.

The energy climb path turns out to be a singular arc control problem that can be analyzed by the Pontryagin's minimum principle.[12] In brief, the minimum principle introduces the concept of Hamiltonian functions in analytical dynamics that must be minimized (or maximized) during a trajectory optimization. The optimization problems are formulated using calculus of variations to determine a set of optimality conditions for a set of adjoint variables that

*Research Scientist, Intelligent Systems Division, Mail Stop 269-1

provide the sensitivity for the control problems.[13] This is known as an indirect optimization method which typically involves a high degree of analytical complexity due to the introduction of the adjoint variables that effectively doubles the number of state variables. Furthermore, the solution method frequently involves solving a two-point boundary value problem. Nonetheless, the adjoint method provides a great degree of mathematical elegance that can reveal the structure of a problem. In some cases, exact analytical optimal solutions can be obtained. Except for simple problems, many trajectory optimization problems require numerical methods that can solve two-point boundary value problems such as gradient-based methods, shooting methods, dynamic programming, etc.

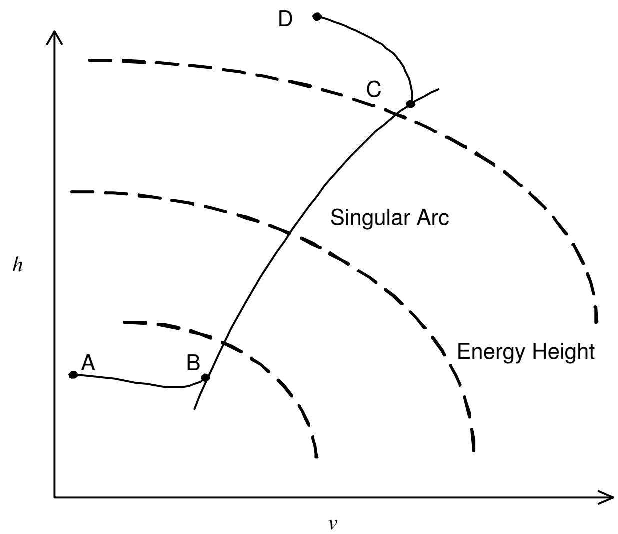

Fig. 1 - Time-Optimal Energy Climb Path

Within the framework of the Pontryagin's minimum principle, the singular-arc optimal control method is an intermediate method for the trajectory optimization. The existence of a singular arc in the time optimal control can simplify the trajectory optimization significantly. Briefly, the singular arc is described by a switching function that minimizes a Hamiltonian function when the Hamiltonian function is linear with respect to a control variable.

In this study, we will examine an aspect of the minimum time-to-climb problem for an aircraft flying in the presence of a two-dimensional atmospheric wind field. An analytical solution for the singular arc is obtained. Wind patterns at a local airport can affect the climb performance of aircraft. While the time-optimal climb problems have been thoroughly studied in flight mechanics, the effect of winds are usually not included in these studies. A solution method of a minimum-time to climb will then be presented for computing a minimum time-to-climb flight trajectory.

II. Singular Arc Optimal Control

In our minimum time-to-climb problem, the aircraft is modeled as a point mass and the flight trajectory is strictly confined in a vertical plane on a non-rotating, flat earth. The change in mass of the aircraft is neglected and the engine thrust vector is assumed to point in the direction of the aircraft velocity vector. In addition, the aircraft is assumed to fly in an atmospheric wind field comprising of both horizontal and vertical components that are altitude-dependent. The horizontal wind component normally comprises a longitudinal and lateral component. We assume that the aircraft motion is symmetric so that the lateral wind component is not included. Thus, the pertinent equations of motion for the problem are defined in its the state variable form as

$$\dot{h} = v \sin\gamma + w_h \tag{1}$$

$$\dot{v} = \frac{T - D - W\sin\gamma}{m} - \dot{w}_x \cos\gamma - \dot{w}_h \sin\gamma \tag{2}$$

$$\dot{\gamma} = \frac{L - W\cos\gamma}{mv} + \frac{\dot{w}_x \sin\gamma - \dot{w}_h \cos\gamma}{v} \tag{3}$$

where h is the altitude, v is the speed, γ is the flight path angle, T is the thrust force, $D = C_D q S$ is the drag force, $L = C_L q S$ is the lift force, W is the aircraft weight, m is the aircraft mass, and $w_x = w_x(h)$ and $w_h = w_h(h)$ are the respective temporal average horizontal and vertical wind field components as functions of the altitude. Thus, the time rate of change of the wind field can be computed as

$$\dot{w}_x = w_x^{'} \dot{h} = w_x^{'} \left(v \sin \gamma + w_h \right) \tag{4}$$

$$\dot{w}_h = w_h^{'} \dot{h} = w_h^{'} \left(v \sin \gamma + w_h \right) \tag{5}$$

where the prime denotes the derivative with respect to the altitude h. The gradient of the wind velocity with respect to the altitude is also called a vertical wind shear.[16]

The problem is now posed as a minimization of the time-to-climb from an initial speed and an initial altitude to a final speed and a final altitude at a final time t_f. To formulate the time-optimal control problem, we consider the following cost function

$$J = \int_0^{t_f} dt \tag{6}$$

subject to state constraints by Eqs. (1)-(3).

The boundary conditions for the problem are the initial and final altitude and airspeed of the aircraft as

$$h(0) = h_0 \qquad h(t_f) = h_f$$

$$v(0) = v_0 \qquad v(t_f) = v_f$$

$$M(h(0), v(0)) = M_0 \qquad M(h(t_f), v(t_f)) = M_f$$

where M is the Mach number as a function of the altitude and airspeed. The flight path angle $\gamma(0)$ or $\gamma(t_f)$ may be free or fixed.

To solve for the time-optimal control problem of Eq. (6), we apply the Pontryagin's minimum principle which can be stated as follows:

Let $x(t) : (0, t) \rightarrow \mathbb{R}^n$ be state variables and $u(t) : (0, t_f) \rightarrow \mathbb{R}^m$ be in a set of admissible control $\mathcal{U}$ that guides a dynamical system described by $\dot{x} = f(x(t), u(t))$ from an initial state $x(0)$ to a final state $x(t_f)$ where $f(x, u) : \mathbb{R}^n \times \mathbb{R}^m \rightarrow \mathbb{R}^n$ is some function, there exist a set of variables $\lambda(t) : (0, t) \rightarrow \mathbb{R}^n$, called adjoint variables, such that we have the following necessary conditions for optimality casted in a Hamiltonian canonical structure

$$\dot{x} = \frac{\partial H(x(t), u(t), \lambda(t))}{\partial \lambda^T} \tag{7}$$

$$\dot{\lambda} = -\frac{\partial H(x(t), u(t), \lambda(t))}{\partial x^T} \tag{8}$$

where $H(x(t), u(t), \lambda(t))$ is the Hamiltonian function of the dynamical system which, for a minimum time-to-climb optimal control problem, is defined as

$$H(x(t), u(t), \lambda(t)) = 1 + \lambda^T(t) f(x(t), u(t)) \tag{9}$$

The optimal control is given by the following necessary condition

$$u^*(t) = \arg \min_{u \in \mathcal{U}} H(x^*(t), u(t), \lambda(t)) \tag{10}$$

If the dynamical system is autonomous, that is f is not an explicit function of time, the Hamiltonian function is required to be zero throughout the optimal solution[6]

$$H(x(t), u(t), \lambda(t)) = 0 \tag{11}$$

A singular control exists if the control variable u appears linearly in the Hamiltonian function H corresponding to[15]

$$\frac{\partial^2 H}{\partial u^2} = 0 \tag{12}$$

Let $S(x,\lambda):\mathbb{R}^n\times\mathbb{R}^n\rightarrow\mathbb{R}^m$ be a switching function defined by

$$S=\frac{\partial H}{\partial u} \tag{13}$$

Since the control u does not appear explicitly in S, it cannot be determined explicitly. However, by differentiating S repeatedly until the control u appears explicitly, then the control u is so determined. For the control u to be optimal, the Kelley's condition must be satisfied

$$(-1)^k\frac{\partial}{\partial u}\left(\frac{d^{2k}S}{dt^{2k}}\right)\geq 0 \tag{14}$$

For this problem, the Hamiltonian function is defined as

$$\begin{aligned}H\left(h,v,\gamma,\lambda_h,\lambda_v,\lambda_\gamma T,C_L,C_D\right)=1+\lambda_h\left(v\sin\gamma+w_h\right)+\lambda_v\left(\frac{T-D-W\sin\gamma}{m}-\dot{w}_x\cos\gamma-\dot{w}_h\sin\gamma\right)\\+\lambda_\gamma\left(\frac{L-W\cos\gamma}{mv}+\frac{\dot{w}_x\sin\gamma-\dot{w}_h\cos\gamma}{v}\right)\end{aligned} \tag{15}$$

where λ_h, λ_v, and λ_γ are the adjoint variables.

We define the specific excess thrust F and the wing loading factor n as functions of the altitude, Mach number M, and Reynolds number Re as

$$F\left(h,v,C_L\right)=\frac{T\left[h,M\left(h,v\right)\right]-\left\{C_{D,0}\left[Re\left(h,v\right)\right]+KC_L^2\right\}q\left[\rho\left(h\right),M\left(h,v\right)\right]S}{W} \tag{16}$$

$$n\left(h,v,C_L\right)=\frac{C_Lq\left[\rho\left(h\right),M\left(h,v\right)\right]S}{W} \tag{17}$$

where $C_{D,0}$ is the profile drag coefficient and K is the induced drag parameter.

Then, the necessary conditions for optimality result in the following adjoint differential equations

$$\begin{aligned}\dot{\lambda}_h=-\frac{\partial H}{\partial h}=-\lambda_h w_h^{'}-\lambda_v\left[g\frac{\partial F}{\partial h}-\left(w_x^{''}\cos\gamma+w_h^{''}\sin\gamma\right)\left(v\sin\gamma+w_h\right)-\left(w_x^{'}\cos\gamma+w_h^{'}\sin\gamma\right)w_h^{'}\right]\\-\lambda_\gamma\left[\frac{g}{v}\frac{\partial n}{\partial h}+\left(w_x^{''}\sin\gamma-w_h^{''}\cos\gamma\right)\left(\sin\gamma+\frac{w_h}{v}\right)+\frac{w_h^{'}\left(w_x^{'}\sin\gamma-w_h^{'}\cos\gamma\right)}{v}\right]\end{aligned} \tag{18}$$

$$\begin{aligned}\dot{\lambda}_v=-\frac{\partial H}{\partial v}=-\lambda_h\sin\gamma-\lambda_v\left[g\frac{\partial F}{\partial v}-\left(w_x^{'}\cos\gamma+w_h^{'}\sin\gamma\right)\sin\gamma\right]\\-\lambda_\gamma\left[\frac{g}{v}\frac{\partial n}{\partial v}-\frac{gn}{v^2}+\frac{g\cos\gamma}{v^2}-\frac{w_h\left(w_x^{'}\sin\gamma+w_h^{'}\cos\gamma\right)}{v^2}\right]\end{aligned} \tag{19}$$

$$\begin{aligned}\dot{\lambda}_\gamma=-\frac{\partial H}{\partial \gamma}=-\lambda_h v\cos\gamma-\lambda_v\left[-g\cos\gamma-v\left(w_x^{'}\cos 2\gamma+w_h^{'}\sin 2\gamma\right)+\left(w_x^{'}\sin\gamma-w_h^{'}\cos\gamma\right)w_h\right]\\-\lambda_\gamma\left[\frac{g\sin\gamma}{v}+w_x^{'}\sin 2\gamma-w_h^{'}\cos 2\gamma+\frac{w_h\left(w_x^{'}\cos\gamma+w_h^{'}\sin\gamma\right)}{v}\right]\end{aligned} \tag{20}$$

In order to determine the extremal control to achieve a fastest climb path, we take the lift coefficient C_L as a control variable. Then the optimal control is one that renders the Hamiltonian stationary

$$\frac{\partial H}{\partial C_L}=-\lambda_v\frac{2KC_L^*qS}{m}+\lambda_\gamma\frac{qS}{mv}=0\Rightarrow C_L^*=\frac{\lambda_\gamma}{2Kv\lambda_v} \tag{21}$$

subject to the inequality constraint $C_{L,min} \leq C_L^* \leq C_{L,max}$.

The optimal lift coefficient in Eq. (21) may be solved by a two-point boundary value problem using a numerical method such as a shooting method or a gradient descent method. Such a numerical solution often does not reveal a structure of the optimal control analytically. In most cases, it is found that this problem can be approximated as a singular optimal control problem by making an assumption that the induced drag parameter K is usually small and therefore can be neglected. In fact, the ideal induced drag parameter for an elliptical wing loading is given by

$$K = \frac{1}{\pi AR} \tag{22}$$

where AR is the aspect ratio. For a typical transport aircraft, the wing aspect ratio is about 7 so that the ideal K parameter is about 0.045. Thus, this assumption is reasonable.

Under this assumption, we see that $\partial^2 H / \partial C_L^2 = 0$ and so there exists a singular control with a switching function

$$S = \lambda_\gamma \frac{qS}{mv} \tag{23}$$

Since $qS/mv > 0$, we then obtain a bang-bang extremal control as

$$C_L^* = \begin{cases} C_{L,max} & \lambda_\gamma < 0 \\ C_{L,sing} & \lambda_\gamma = 0 \\ C_{L,min} & \lambda_\gamma > 0 \end{cases} \tag{24}$$

The bang-bang control law is thus viewed as a sub-optimal solution to the minimum time optimal control problem. Equation (24) states that the minimum-time-to-climb trajectory is approximated by three sub-optimal arcs. The first arc is a trajectory on which the aircraft flies at some initial altitude and airspeed at a maximum lift coefficient until it intercepts with a singular arc trajectory defined by the second switching condition. The singular arc is an optimal flight trajectory for the fastest climb[8] and is also called an energy climb path (ECP) since it is a path that crosses a set of level curves of constant energy heights $E = h + v^2/2g$ as illustrated in Fig. 1. At some point on this trajectory, the aircraft climbs out of the singular arc and flies along a final arc with a minimum lift coefficient to arrive at the final altitude and airspeed.

To find a singular control, we use the fact that $S = 0$ and $\dot{S} = 0$ on the singular arc to establish that $\lambda_\gamma = 0$ and $\dot{\lambda}_\gamma = 0$. Hence, this allows us to eliminate λ_γ in Eq. (20) by solving for λ_h

$$\lambda_h = \lambda_v \left[\frac{g}{v} + \frac{w_x^{'} \cos 2\gamma + w_h^{'} \sin 2\gamma}{\cos\gamma} - \frac{w_h \left(w_x^{'} \tan\gamma - w_h^{'} \right)}{v} \right] \tag{25}$$

The remaining adjoint equations (18) and (19) now become

$$\dot{\lambda}_h = \lambda_v \left\{ -g \left(\frac{\partial F}{\partial h} + \frac{w_h^{'}}{v} \right) + \left[w_x^{'} w_h^{'} \tan\gamma + w_x^{''} v \cos\gamma + w_h^{''} v \sin\gamma - \left(w_h^{'} \right)^2 \right] \left(\sin\gamma + \frac{w_h}{v} \right) \right\} \tag{26}$$

$$\dot{\lambda}_v = \lambda_v \left[-g \left(\frac{\partial F}{\partial v} + \frac{\sin\gamma}{v} \right) + \sin\gamma \left(w_x^{'} \tan\gamma - w_h^{'} \right) \left(\sin\gamma + \frac{w_h}{v} \right) \right] \tag{27}$$

Differentiating Eq. (25), which is equivalent to computing $\ddot{S} = \ddot{\lambda}_\gamma$, and then substituting Eq. (27) into the resulting expression yield

$$\dot{\lambda}_h = \lambda_v \left\{ \frac{gF}{v^2} \left[-g + \left(w_x^{'} \tan\gamma - w_h^{'} \right) w_h \right] - g \frac{\partial F}{\partial v} \left[\frac{g}{v} + \frac{w_x^{'} \cos 2\gamma + w_h^{'} \sin 2\gamma}{\cos\gamma} - \frac{w_h \left(w_x^{'} \tan\gamma - w_h^{'} \right)}{v} \right] \right.$$
$$+ \frac{gn}{v} \left[-w_x^{'} \sin\gamma \left(3 + \tan^2\gamma \right) + 2 w_h^{'} \cos\gamma - \frac{w_x^{'} w_h}{v \cos^2\gamma} \right] + \frac{g}{v} \left(3 w_x^{'} \tan\gamma - 2 w_h^{'} + \frac{2 w_x^{'} w_h}{v \cos\gamma} \right)$$
$$+ \left[-\frac{2 \left(w_x^{'} \right)^2 \tan\gamma}{\cos\gamma} \left(\sin\gamma + \frac{w_h}{v} \right) + \frac{w_x^{'} w_h^{'}}{\cos\gamma} \left(3 \sin\gamma + 2 \frac{w_h}{v} \right) - \left(w_h^{'} \right)^2 \right] \left(\sin\gamma + \frac{w_h}{v} \right)$$
$$\left. + \left[\frac{w_x^{''} \cos 2\gamma + w_h^{''} \sin 2\gamma}{\cos\gamma} - \frac{w_h \left(w_x^{''} \tan\gamma - w_h^{''} \right)}{v} \right] \left(\sin\gamma + \frac{w_h}{v} \right) \right\} \quad (28)$$

By equating Eq. (28) to Eq. (26), the singular arc for a minimum time-to-climb is now obtained as

$$f(h, v, \gamma, n) = (1 - a_1) F + (1 + a_2) v \frac{\partial F}{\partial v} - \frac{v^2}{g} \frac{\partial F}{\partial h} + a_3 n + a_4 = 0 \quad (29)$$

with the coefficients a_1, a_2, a_3, and a_4 described by the following functions of the wind field parameters

$$a_1 = \frac{w_h \left(w_x^{'} \tan\gamma - w_h^{'} \right)}{g} \quad (30)$$

$$a_2 = \frac{v \left(w_x^{'} \cos 2\gamma + w_h^{'} \sin 2\gamma \right)}{g \cos\gamma} - \frac{w_h \left(w_x^{'} \tan\gamma - w_h^{'} \right)}{g} \quad (31)$$

$$a_3 = \frac{v}{g} \left[w_x^{'} \sin\gamma \left(3 + \tan^2\gamma \right) - 2 w_h^{'} \cos\gamma + \frac{w_x^{'} w_h}{v \cos^2\gamma} \right] \quad (32)$$

$$a_4 = \left(\frac{v \sin\gamma + w_h}{g} \right)^2 \left[\frac{2 w_x^{'} \left(w_x^{'} \tan\gamma - w_h^{'} \right)}{\cos\gamma} + v \left(w_x^{''} \tan\gamma - w_h^{''} \right) \right] - \frac{v}{g} \left(3 w_x^{'} \tan\gamma - w_h^{'} + \frac{2 w_x^{'} w_h}{v \cos\gamma} \right) \quad (33)$$

Equation (29) is a partial differential equation in terms of the specific excess thrust F that describes an optimal climb path for a minimum time-to-climb solution for an aircraft flying in the presence of an altitude dependent atmospheric wind field. Examining Eq. (29) reveals that there is a high degree of cross coupling between the horizontal wind field and the vertical wind field up to the second derivatives of the wind fields. Thus, not only the wind field gradients affect the optimal climb path, but the wind field curvatures also play a role as well. Equation (29) results in a parabolic equation in terms of C_L, which can be solved to give a feedback control for the lift coefficient on the singular arc as a function of the three state variables h, v, and γ.

A certain simplification of Eq. (29) can be made by considering the concept of fast and slow states in flight dynamics. Ardema had shown that in optimal trajectory analysis, the three-state model of a point mass aircraft exhibits a time-scale separation behavior whereby the state variables h and v possess slower dynamics than the state variable γ.[3] This time scale separation is normally treated by a singular perturbation analysis by replacing the fast state equation with the following equation

$$\epsilon \dot{\gamma} = \frac{L - W \cos\gamma}{mv} + \frac{\dot{w}_x \sin\gamma - \dot{w}_h \cos\gamma}{v} \quad (34)$$

where ϵ is a small parameter.

Equation (34) has an inner solution and an outer solution, which is the steady state solution obtained by setting $\epsilon = 0$. The inner solution can usually be solved by the method of matched asymptotic expansion. The inner solution is also called a boundary-layer solution in reference to the historical origin of the singular perturbation method in the fluid boundary layer theory. The overall solution is dominated by the outer solution with the inner solution only affecting a small initial time period. As a first order approximation, the inner solution can sometimes be ignored. In this case, Eq. (34) results in the following load factor

$$n = \cos\gamma - \frac{(v\sin\gamma + w_h)\left(w_x^{'}\sin\gamma - w_h^{'}\cos\gamma\right)}{g} \tag{35}$$

Equation (35) thus dethrones the number of state equations from three to two by converting the state variable γ into a control variable in place of the lift coefficient C_L. Substituting Eq. (35) into Eq. (29) now yields the optimal climb path function

$$\begin{aligned} f(h,v,\gamma) = F\left[1 - \frac{w_h\left(w_x^{'}\tan\gamma - w_h^{'}\right)}{g}\right] + v\frac{\partial F}{\partial v}\left[1 + \frac{v\left(w_x^{'}\cos 2\gamma + w_h^{'}\sin 2\gamma\right)}{g\cos\gamma} - \frac{w_h\left(w_x^{'}\tan\gamma - w_h^{'}\right)}{g}\right] \\ - \frac{v^2}{g}\frac{\partial F}{\partial h} - \frac{v}{g}\left(2w_x^{'}\sin^2\gamma\tan\gamma + w_h^{'}\cos 2\gamma + \frac{w_x^{'}w_h}{v\cos\gamma}\right) + v\left(\frac{v\sin\gamma + w_h}{g}\right)^2\left(w_x^{''}\tan\gamma - w_h^{''}\right) \\ + \frac{v}{g}\left(\frac{v\sin\gamma + w_h}{g}\right)\left(w_x^{'}\tan\gamma - w_h^{'}\right)\left(-w_x^{'}\tan\gamma\cos 2\gamma + 2w_h^{'}\cos^2\gamma + \frac{w_x^{'}w_h}{v\cos\gamma}\right) = 0 \end{aligned} \tag{36}$$

We have thus reduced the optimal climb path by removing the dependency on the lift coefficient. We now examine some special cases of the general optimal climb path function $f(h,v,\gamma)$:

1. Steady Wind Field:
   For a steady wind field, the gradients and curvatures vanish, thereby reducing the optimal climb path function to the following

$$f(h,v) = F + v\frac{\partial F}{\partial v} - \frac{v^2}{g}\frac{\partial F}{\partial h} = 0 \tag{37}$$

   Equation (37) is the well-known result for the ECP without an atmospheric wind field. Thus, the optimal climb path in the presence of a steady wind field is effectively the same as that without the wind field effect. This result is not surprising and can be explained by the fact that since the inertial reference frame is attached to the air mass, whether the air mass is moving at a constant speed or remains stationary, the speed of the aircraft relative to the air mass is the same, thus resulting in the same optimal climb path.

2. Horizontal Wind Field:
   In the presence of a horizontal wind field only, the optimal climb path function becomes

$$\begin{aligned} f(h,v,\gamma) = F + v\frac{\partial F}{\partial v}\left(1 + \frac{vw_x^{'}\cos 2\gamma}{g\cos\gamma}\right) - \frac{v^2}{g}\frac{\partial F}{\partial h} - \frac{2vw_x^{'}\sin^2\gamma\tan\gamma}{g} + \frac{v^3w_x^{''}\sin^2\gamma\tan\gamma}{g^2} \\ - \frac{v^2\left(w_x^{'}\right)^2}{g^2}\sin\gamma\tan^2\gamma\cos 2\gamma = 0 \end{aligned} \tag{38}$$

   Specializing Eq. (38) for small flight path angles by invoking $\sin\gamma \approx \gamma$ and $\cos\gamma \approx 1$ yields

$$f(h,v) = F + v\frac{\partial F}{\partial v}\left(1 + \frac{vw_x^{'}}{g}\right) - \frac{v^2}{g}\frac{\partial F}{\partial h} - \left[\frac{2vw_x^{'}}{g} - \frac{v^3w_x^{''}}{g^2} + \frac{v^2\left(w_x^{'}\right)^2}{g^2}\right]\gamma^3 = 0 \tag{39}$$

3. Vertical Wind Field:

In the presence of a vertical wind field only, Eq. (36) becomes

$$f(h,v,\gamma) = F\left(1+\frac{w_h w_h^{'}}{g}\right) + v\frac{\partial F}{\partial v}\left(1+\frac{v w_h^{'}\sin 2\gamma}{g\cos\gamma}+\frac{w_h w_h^{'}}{g}\right) - \frac{v^2}{g}\frac{\partial F}{\partial h} - \frac{v w_h^{'}\cos 2\gamma}{g}$$
$$- v w_h^{''}\left(\frac{v\sin\gamma + w_h}{g}\right)^2 - \frac{2v\left(w_h^{'}\right)^2\cos^2\gamma}{g}\left(\frac{v\sin\gamma + w_h}{g}\right) = 0 \quad (40)$$

For small flight path angles, Eq. (40) reduces to

$$f(h,v,\gamma) = F\left(1+\frac{w_h w_h^{'}}{g}\right) + v\frac{\partial F}{\partial v}\left(1+\frac{2v w_h^{'}\gamma + w_h w_h^{'}}{g}\right) - \frac{v^2}{g}\frac{\partial F}{\partial h} - \frac{v w_h^{'}}{g} - v w_h^{''}\left(\frac{v\gamma + w_h}{g^2}\right)^2$$
$$- \frac{2v\left(w_h^{'}\right)^2}{g}\left(\frac{v\gamma + w_h}{g}\right) = 0 \quad (41)$$

Vertical wind field is especially important for microburst problems. A microburst is a wind shear disturbance characterized by an unusually strong downdraft near the ground surface that presents an extreme hazard to aircraft during take-off or landing.

III. Optimal Solution

During a climb, the aircraft flies under a maximum continuous thrust from take-off to a point in the flight trajectory envelope where it intersects with the optimal climb path. The aircraft then maintains its course along the optimal climb path until it reaches some point on the optimal climb path where it climbs out to the final altitude and airspeed. Thus, there exist three climb segments during a climb as illustrated in Fig. 1 labeled as A, B, and C where B is the singular arc optimal climb path. The suboptimal solutions for the climb segments A and C may be defined by lines of constant energy heights $E = h + v^2/2g$.[11]

From the optimal control perspective, the initial and final climb segments are to be determined by requiring the Hamiltonian function as defined in Eq. (15) to be zero. In addition, the adjoint variable λ_γ is no longer restricted to zero according to the first and last switching conditions in Eq. (24). Thus, in general, the optimal solutions for the initial and final flight segments are considerably more complex than the optimal climb path solution and usually involve solving a two-point boundary value problem.

First, we shall consider the singular arc optimal solution. Along this singular arc, all the state and adjoint variables are functions of the altitude h, airspeed v, and flight path angle γ. However, it can easily be shown that the flight path angle γ on the singular arc optimal energy climb path is in turn a function of the altitude h and airspeed v. Therefore, the two variables h and v uniquely determine the optimal climb path. In particular, for the case of small flight path angles for which Eqs. (39) and (41) apply. The optimal climb function $f(h,v,\gamma)$ can be written as

$$f(h,v,\gamma) = \sum_{n=0}^{3} f_i(h,v)\,\gamma^i = 0 \quad (42)$$

where f_i are explicit functions of v and h.

The time derivative of $f(h,v,\gamma)$ is evaluated as

$$\dot{f} = \sum_{i=0}^{3}\left(\frac{\partial f_i}{\partial h}\dot{h} + \frac{\partial f_i}{\partial v}\dot{v}\right)\gamma^i \quad (43)$$

taking into account that the assumption $\dot{\gamma} = 0$ is built into the climb path function.

Substituting Eqs. (1)-(3) into Eq. (43) then yields the following polynomial equation that can be solved for the flight path angle γ

$$c_5\gamma^5 + c_4\gamma^4 + \sum_{i=0}^{3} c_i(h,v)\,\gamma^i = 0 \quad (44)$$

where the coefficients c_i are

$$c_5(h,v) = -\frac{\partial f_3}{\partial v} v w_h^{'} \tag{45}$$

$$c_4(h,v) = \frac{\partial f_3}{\partial h} v - \frac{\partial f_3}{\partial v}\left(v w_x^{'} + w_h w_h^{'} + g\right) - \frac{\partial f_2}{\partial v} v w_h^{'} \tag{46}$$

$$c_i(h,v) = \frac{\partial f_i}{\partial h} w_h + \frac{\partial f_i}{\partial v}\left(Fg - w_h w_x^{'}\right) + \frac{\partial f_{i-1}}{\partial h} v - \frac{\partial f_{i-1}}{\partial v}\left(v w_x^{'} + w_h w_h^{'} + g\right) - \frac{\partial f_{i-2}}{\partial v} v w_h^{'} \tag{47}$$

Equation (44) gives the flight path angle as a function of the altitude and speed. Thus the optimal climb surface function $f(h,v,\gamma)$ can be replaced by a climb path function $f(h,v,\gamma(h,v))$ upon embedding the solution of the flight path angle from Eq. (44).

The adjoint variables along the optimal climb path are now determined from enforcing the conditions $H=0$ and $\lambda_\gamma = 0$ on the singular arc as

$$\lambda_h = -\frac{g + v w_x^{'} + 2 v w_h^{'}\gamma - w_h w_x^{'}\gamma + w_h w_h^{'}}{gv(F-\gamma) + (v\gamma + w_h)\left(g + v w_h^{'}\gamma - w_h w_x^{'}\gamma + w_h w_h^{'}\right)} \tag{48}$$

$$\lambda_v = -\frac{v}{gv(F-\gamma) + (v\gamma + w_h)\left(g + v w_h^{'}\gamma - w_h w_x^{'}\gamma + w_h w_h^{'}\right)} \tag{49}$$

The foregoing analysis has shown that the along the singular arc, the time optimal trajectory is known in the $v-h$ plane as well as the flight path angle and the adjoint variables. This information greatly facilitates the optimal solutions for the climb segments on the initial and final arcs. Since the initial conditions on the initial climb segment are known according to the problem statement and the fact that its solution must terminate on the optimal climb path function for which all the state and adjoint variables are known, then the optimal solution for the initial arc can be computed using a shooting technique to integrate backward from some point B on the optimal climb path to the initial point A as shown in Fig. 1. Likewise, to compute the optimal solution for the final arc, a shooting method may be used to integrate forward from some point C on the optimal climb path to the final point D that terminates at the desired altitude and airspeed. A shooting method may be established as follows:

The flight path angle γ not on the optimal climb path function can be solved by setting the Hamiltonian in Eq. (15) to zero with the usual small angle assumption, thus resulting in the following quadratic equation

$$\lambda_v v w_h^{'}\gamma^2 + \left[\lambda_h v - \lambda_v\left(g + v w_x^{'} - w_h w_h^{'}\right)\right]\gamma + 1 + \lambda_h w_h + \lambda_v\left(Fg - w_h w_x^{'}\right) = 0 \tag{50}$$

Equation (50) is then used to eliminate the flight path angle expression in the adjoint equation in the adjoint differential equations (18) and (19), which can then be parameterized in terms of the altitude as the independent variable instead of time using the following transformation with the small angle assumption

$$\frac{d\lambda_h}{dh} = \frac{\dot{\lambda}_h}{\dot{h}} = \frac{-\lambda_h w_h^{'} - \lambda_v\left[g\frac{\partial F}{\partial h} - \left(w_x^{''} + w_h^{''}\gamma\right)(v\gamma + w_h) - \left(w_x^{'} + w_h^{'}\gamma\right)w_h^{'}\right]}{v\gamma + w_h} \tag{51}$$

$$\frac{d\lambda_v}{dv} = \frac{\dot{\lambda}_v}{\dot{h}} = \frac{-\lambda_h\gamma - \lambda_v\left[g\frac{\partial F}{\partial v} - \left(w_x^{'} + w_h^{'}\gamma\right)\gamma\right]}{v\gamma + w_h} \tag{52}$$

In addition, the airspeed can also be parameterized as a function the altitude as

$$\frac{dv}{dh} = \frac{\dot{v}}{\dot{h}} = \frac{(F-\gamma)g}{v\gamma + w_h} - w_x^{'} + w_h^{'}\gamma \tag{53}$$

Equations (50)-(53) are then integrated either forward or backward using the known state and adjoint variables on the optimal climb path as the starting values at points B and C. The shooting method then iterates on these known values on the optimal climb path until the conditions at points A and D are met.

IV. Numerical Example

We compute the time optimal climb trajectory of a transport aircraft in a horizontal wind field. The aircraft has a maximum thrust T_{max} which varies as a function of the altitude as

$$T = T_{max}\left(\frac{\rho}{\rho_0}\right)^a \tag{54}$$

where ρ is the density, ρ_0 is the density at the sea level, and a is a constant.

Using Eq. (35) with the small flight path angle approximation, the specific excess thrust is computed as

$$F = \frac{T_{max}}{W}\left(\frac{\rho}{\rho_0}\right)^a - \frac{C_D\frac{1}{2}\rho v^2 S}{W} \tag{55}$$

The optimal climb path function, Eq. (39), is equal to

$$f(v,h) = \frac{T_{max}}{W}\left(\frac{\rho}{\rho_0}\right)^a\left(1-\frac{av^2}{\rho g}\frac{d\rho}{dh}\right) - \frac{C_D\frac{1}{2}\rho v^2 S}{W}\left(2-\frac{v^2}{\rho g}\frac{d\rho}{dh}+\frac{2vw_x^{'}}{g}\right) - \left[\frac{2vw_x^{'}}{g}-\frac{v^3w_x^{''}}{g^2}+\frac{v^2\left(w_x^{'}\right)^2}{g^2}\right]\gamma^3 = 0 \tag{56}$$

The aircraft has the following values: T_{max} =40000 lb, W =200000 lb, S =1591 ft^2, $C_D = 0.0343$, and $a = 0.7$.

We will compute the singular arc for two typical horizontal wind field problems. The first wind field problem is a low-altitude wind shear disturbance described by the following model

$$w_x = a_1e^{-\frac{h}{h_1}} - a_2e^{-\frac{h}{h_2}} \tag{57}$$

where, for the problem, $a_1 = 250$ ft/sec, $a_2 = 200$ ft/sec, $h_1 = 6000$ ft, and $h_2 = 1000$ ft.

The second wind field problem is a high-altitude wind field problem described by the following power law model

$$w_x = a_3\left(\frac{h-h_3}{h_4}\right)^\alpha \tag{58}$$

where, for the problem, $a_3 = 250$ ft/sec, $h_3 = -1000$ ft/sec, $h_4 = 30000$ ft, and $\alpha = \frac{1}{7}$.

The two types of wind field are plotted in Fig. 2.

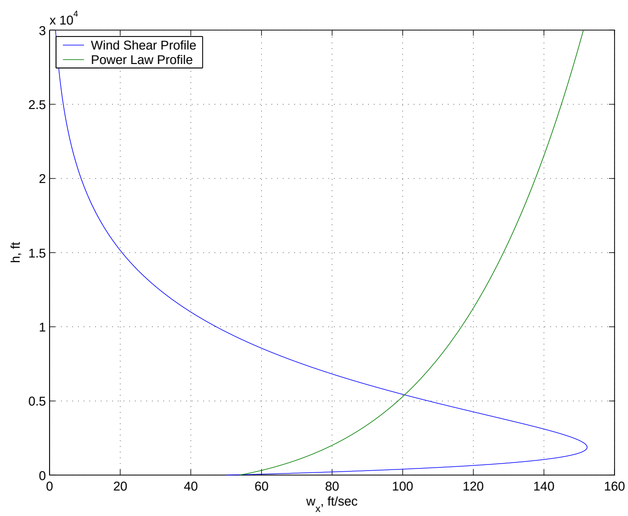

Fig. 2 - Wind Shear and Power Law Models

As can seen, the wind shear profile is characterized by a strong wind field gradient near the ground which can be hazardous to aircraft during take-off and landing.

To find the singular arc, we decompose the optimal climb path function, Eq. (56), in the individual functions $f_i(h, v)$ according to Eq. (42). For a horizontal wind field problem, Eq. (44) is then formulated as a 4^{th} degree polynomial function in terms of the flight path angle γ. A physically correct root is obtained that yields the flight path angle on the singular arc. The singular arc function $f(h, v)$ then becomes a nonlinear function in terms of h and v. To compute the singular arc trajectory in the $v - h$ plane, we find the zero solution of this function using a Newton-Raphson method as follows:

$$v_{i+1} = v_i - \left[\frac{df(h_i, v_i)}{dv}\right]^{-1} f(h_i, v_i) \tag{59}$$

The computed singular arc time-optimal climb paths for both wind field profiles are plotted in Fig. 3. For reference, we also compute the singular arc for zero wind disturbance. As can be seen, the singular arc climb paths are steep paths that rapidly increase the altitude with a relatively smaller change in the air speed for the case of no wind. The power law profile follows a similar pattern as the no-wind case, although the ground speed intercept is less. This would mean that with the power law profile, the aircraft has to enter the singular arc climb path at lower speed than if there were no wind. The singular arc for the wind shear profile is the most interesting in that the speed variation is significant over a wide range at a very low altitude. This is due to the strong wind field gradient over a short altitude. At high altitude, the three singular arcs are converging, so the effect of wind field is less pronounced at high altitude.

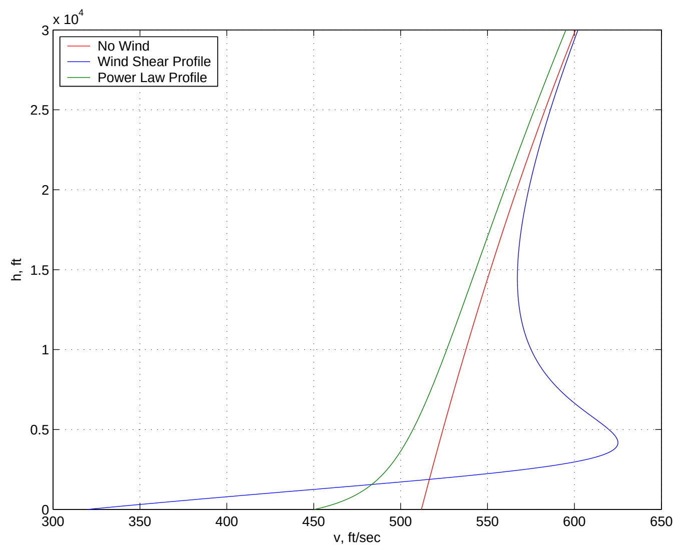

Fig. 3 - Singular Arc Time-Optimal Climb Paths

Once the singular arc has been determined, the values of h and v along the singular arc are plugged into the 4^{th} degree polynomial to solve for the flight path angle along the singular arc. The lift coefficients are also computed. Figs. 4 and 5 are the plots of the flight path angle and lift coefficient on the singular arc climb paths. The flight path angle for the no-wind case generally decreases with altitude. At high altitude, the flight path angle for the two wind profiles converge to that of the no-wind case. The wind shear case as usual shows a drastic change in the flight path angle along the singular arc at low altitude. The lift coefficient generally increases with altitude for the no-wind case. The lift coefficient for the wind shear case varies greatly at very low altitude and is quite large at ground level due to the low ground speed intercept required to enter the climb path.

We next compute a complete trajectory from take-off to some final altitude and air speed. We only consider the wind shear case. The initial ground speed at take-off is about Mach 0.2 or 224 ft/sec and the desired air speed at 15000 ft is Mach 0.5 and 0.6. The solutions not on singular arc require solving a two-point boundary value problem. However, since the adjoint variables are completely determined on the singular arc, we can solve the trajectory off the singular arc quite easily using a shooting method by integrating Eqs. (51) to (53) either forward or backward starting from the singular arc. The adjoint solution on the singular arc is plotted in Fig. 6.

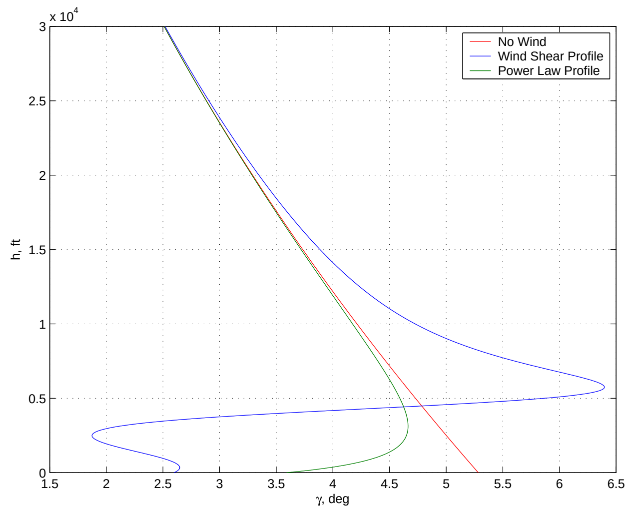

Fig. 4 - Flight Path Angle on Singular Arc

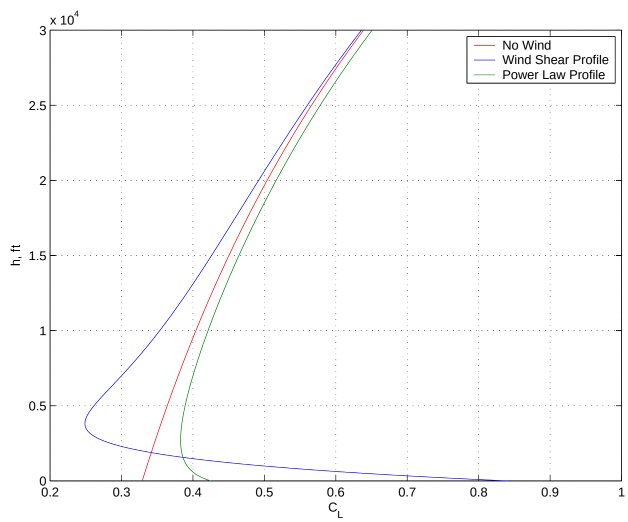

Fig. 5 - Lift Coefficient on Singular Arc

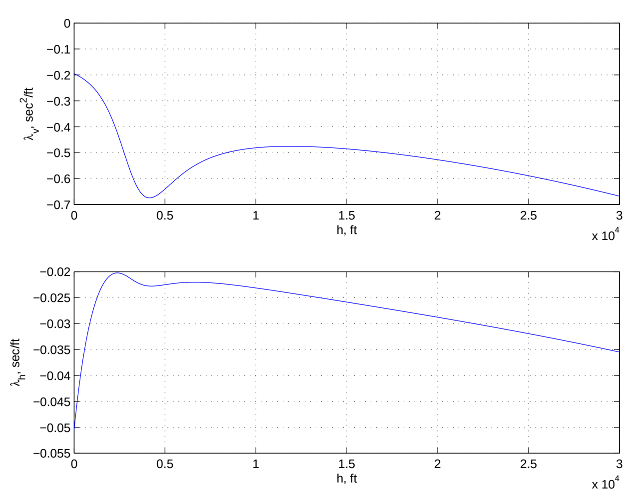

Fig. 6 - Adjoint Solution on Singular Arc

The complete trajectory is plotted in Fig. 7. To climb to 15000 ft and Mach 0.5, the climb trajectory is comprised of three segments. The first segment, segment AB, is the take-off segment on which the aircraft flies from take-off ground speed to intercept the singular arc at point B. This occurs at a very low altitude. The second segment, or singular arc segment BC, is the minimum-time to climb path that takes the aircraft to a higher altitude in a fastest time. At some point on this singular arc, the aircraft begins to depart at point C and flies on the final segment, segment CD, to the final altitude and airspeed. We note that the three segments join together and are tangent at points B and C. On this path, the departure slope is to the left of the singular arc. In the region to the left of the singular arc, because the altitude is continuously increasing, the thrust is maintained at the maximum value.

The situation for Mach 0.6 corresponding to the final segment EF is different. Since the aircraft must arrive at Mach 0.6 which is to the right of the singular arc. Because the departure slope must be tangent to the singular arc and curve to the left, there is no point below the final altitude where this tangency exists. As a result, the aircraft must fly past the final altitude and then reduce the engine thrust to let the potential energy be convert to kinetic energy once the aircraft begins to slow down. For the problem, we use a first-order model to describe the engine thrust reduction from the maximum value to an idle value at roughly 20% of the maximum thrust. The segment EF is sub-optimal in that the engine thrust varies so that it becomes a control variable in addition to the flight path angle. Nonetheless, it is a very good approximation since the segment EF approximately follows a total energy curve.

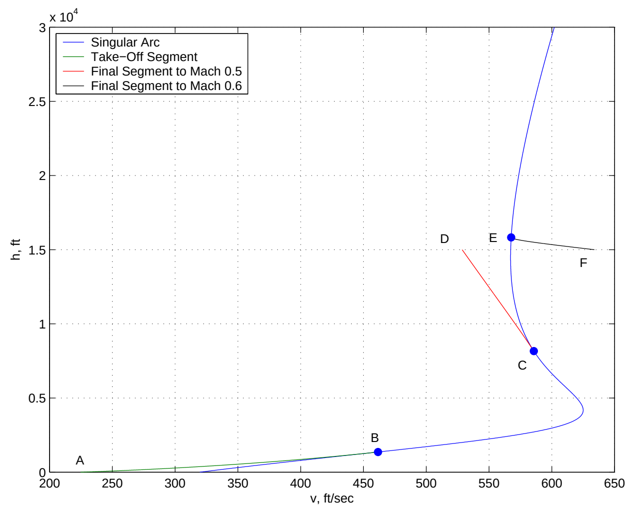

Fig. 7 - Climb Trajectory

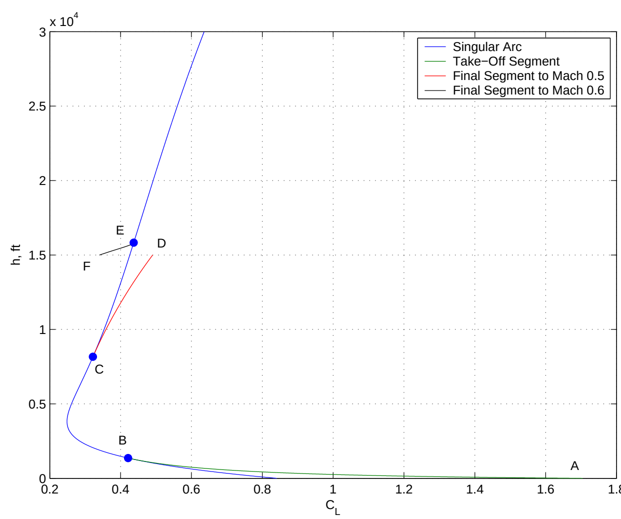

Fig. 8 - Lift Coefficient on Climb Trajectory

The lift coefficient variation on the climb trajectory is shown in Fig. 8. The lift coefficient varies greatly from a maximum take-off value to about 0.4 at a very low altitude. Depending on the wind shear profile, this may not be feasible due to the slow retraction of flaps and slats deployed during take-off. The flight path angle on the climb trajectory is plotted in Fig. 9. The flight path angle for the initial segment AB and the final segment CD are computed using Eq. (50) as a function of the adjoint solution computed from the shooting method. It turns out that the computed flight path angle is very nearly constant as shown in Fig. 10. Thus, an approximate trajectory can easily be computed by only integrating Eq. (53) using a constant flight path angle at a point of tangency to the singular arc. The final segment EF is computed using this approach.

To examine the optimality of the computed solution, we compute the values of the Hamiltonian function along various climb segments. The segments AB, BC, and CD are optimal so the values of the Hamiltonian function are equal to zero. The climb segment EF is sub-optimal and that fact is clearly illustrated by the non-zero value of the Hamiltonian function. Nonetheless, it is a reasonable approximate solution, given that the problem would have been formulated with the engine thrust as an additional control variable, which would result in a more complex problem.

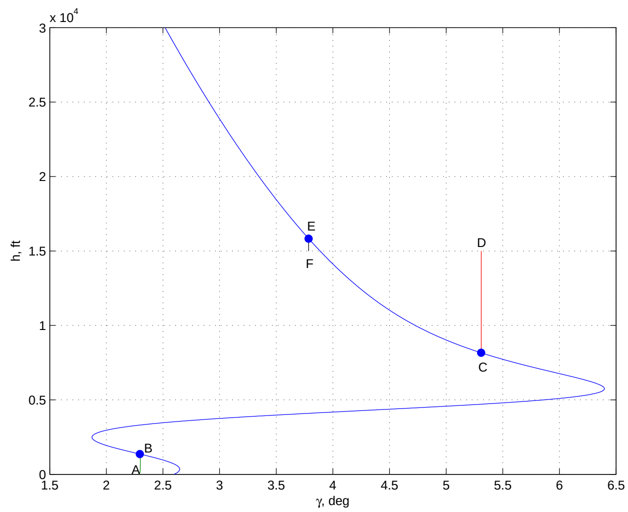

Fig. 9 - Flight Path Angle on Climb Trajectory

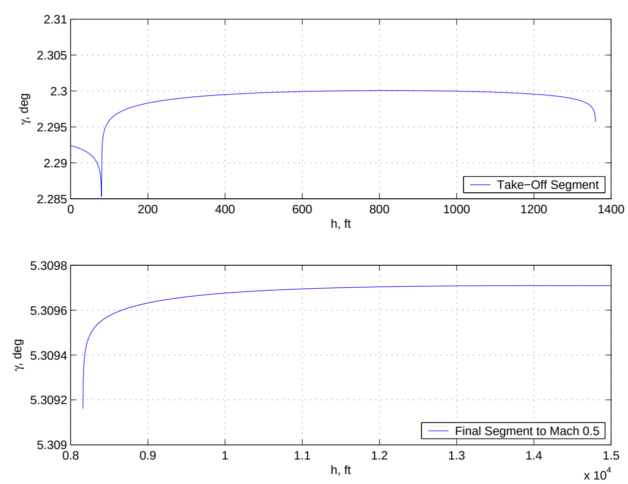

Fig. 10 - Flight Path Angle Computation

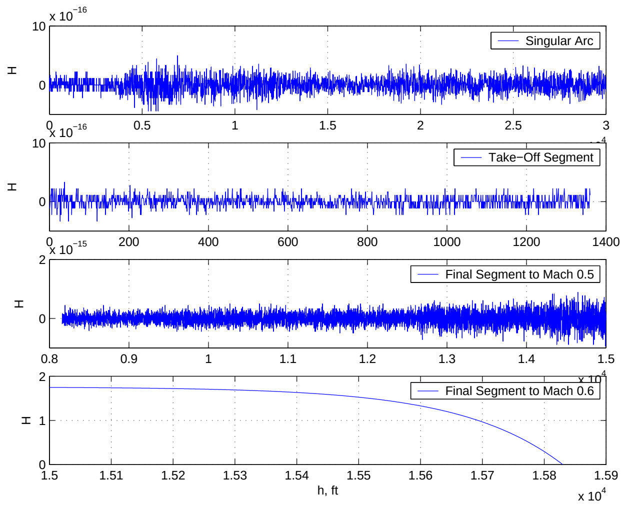

Fig. 11 - Values of Hamiltonian Function

V. Conclusions

A solution to a minimum time-to climb problem in an altitude dependent two-dimensional wind field has been presented. This problem possesses a singular control structure when the lift coefficient is taken as a control variable with the induced drag effect neglected. The optimal climb path on the singular arc is obtained as a function of the three flight state variables and the lift coefficient as a control. A time-scale separation is used to reduce the dimensionality of the optimal climb path function by converting the lift coefficient control into the flight path angle control. Using the singular arc analysis, this three-dimensional function can be further decomposed into a solution for the optimal flight path angle and a two-dimensional climb trajectory as a function of the airspeed and altitude. The known adjoint variables on this optimal trajectory significantly simplifies the general optimal control solution for the initial and final climb segments. A shooting method is formulated to solve numerically the trajectories of the initial and final segments using the known solutions on the optimal climb trajectory. A numerical example for a wind shear profile is computed to demonstrate the analytical method. It is found that the computed flight path angle off the singular arc is nearly a constant and therefore can be used as a very good approximation. The analytical approach provides a rapid means for estimating climb trajectory of aircraft flying in the presence of atmospheric wind.

References

[1] Parsons, M.G., Bryson, A.E., Jr., and Hoffman, W. C., "Long-Range Energy-State Maneuvers for Minimum Time to Specified Terminal Conditions", 11th AIAA Aerospace Sciences Meeting, Washington, D.C., AIAA-1973-229, January 1973.

[2] Breakwell, J.V., "Optimal Flight-Path-Angle Transitions in Minimum Time Airplane Climbs", American Institute of Aeronautics and Astronautics and American Astronautical Society, Astrodynamics Conference, San Diego, CA, AIAA-1976-795, August 1976.

[3] Ardema, M.D., "Solution of the Minimum Time-to-Climb Problem by Matched Asymptotic Expansions", AIAA Journal of Guidance, Control, and Dynamics, Vol. 14, No. 7, 1976, pp. 843-850.

[4] Kelley, H.J., Cliff, E.M., and Visser, H.G., "Energy Management of Three-Dimensional Minimum-Time Intercept", Journal of Guidance, Control, and Dynamics, Vol.10, No. 6, 1987, pp. 574-580.

[5] Ardema, M.D., "Linearization of the Boundary-Layer Equations of the Minimum Time-to-Climb Problem", Journal of Guidance, Control, and Dynamics, Vol. 2, No. 5, 1979, pp. 434-436.

[6] Hedrick, J.K. and Bryson, A.E., Jr., "Three-Dimensional Minimum-Time Turns for a Supersonic Aircraft", Journal of Aircraft, Vol. 9, No. 2, 1972, pp. 115-121.

[7] Bryson, A.E., Jr. and Slattery, R.A., "Minimum-Time Motions of a Two-Arm Robot", AIAA Guidance, Navigation and Control Conference, Portland, OR, August 1990.

[8] Subchan and Zbikowski, R., Cranfield University, "Minimum-Time Optimal Trajectories for Terminal Bunt Manoeuvre", AIAA Guidance, Navigation, and Control Conference, AIAA 2005-5968, August 2005.

[9] Titus, H., Cooper, C.R., and Fallon, M.P., "Minimum Time and Fuel and Sliding Mode Controllers for Spacecraft Attitude Control", Space Programs and Technologies Conference, Huntsville, AL, AIAA-1994-4589, September 1994.

[10] Albassam, B.A., "Optimal Near-Minimum-Time Control Design for Flexible Structures“, Journal of Guidance, Control, and Dynamics, Vol. 25, No. 4, 2002, pp. 618-625).

[11] Vinh, N.X., *Flight Mechanics of High-Performance Aircraft*, Cambridge University Press, 1993.

[12] Pontryagin, L., Boltyanskii, U., Gamkrelidze, R., and Mishchenko, E., *The Mathematical Theory of Optimal Processes*, Interscience, 1962.

[13] Leitmann, G., *The Calculus of Variations and Optimal Control*, Springer, 2006.

[14] Naidu, D.S. and Calise, A.J., "Singular Perturbations and Time Scales in Guidance and Control of Aerospace Systems: A Survey", Journal of Guidance, Control, and Dynamics, Vol. 24, No. 6, 2001, pp. 1057-1078.

[15] Bryson, A., and Ho, Y., *Applied Optimal Control: Optimization, Estimation, and Control*, Hemisphere Publishing Co., 1975.

[16] Nelson, R.C., *Flight Stability and Automatic Control*, McGraw-Hill, 1997.